Check for updates

Mobile monitoring reveals the importance of non-vehicular particulate matter sources in London†

Samuel Wilson, [ID] *[a] Naomi J. Farren, [ID] [a] Shona E. Wilde,[a] Rebecca L. Wagner,[a] James D. Lee, [ID] [a] Lauren E. Padilla, [ID] [b] Greg Slater,[c] Daniel Peters[b] and David. C. Carslaw[ad]

This study uses mobile monitoring to gain a better understanding of particulate matter (PM) sources in two areas of Central and Outer London, UK. We find that, unlike emissions of nitrogen oxides (NO + NO$_2$ = NO$_x$), which are elevated in Central London due to the high number of diesel vehicles and congestion, fine particulate matter (PM$_{2.5}$) emissions are well-controlled. This finding provides evidence for the effectiveness of vehicle particulate filters, supporting the view that their widespread adoption has mitigated PM$_{2.5}$ emissions, even in the highly dieselized area of Central London. However, mobile monitoring also reveals infrequent elevated PM$_{2.5}$ concentrations caused by malfunctioning vehicles. These events were confirmed through simultaneous measurements of PM$_{2.5}$ and sulfur dioxide (SO$_2$), the latter being a strong tracer of engine lubricant combustion. A single event from a gasoline car, representing just 0.15% of the driving distance in Outer London, was responsible for 7.4% of the ΔPM$_{2.5}$ concentration above background levels, highlighting the ongoing importance of addressing high-emission vehicles. In a novel application of mobile monitoring, we demonstrate the ability to identify and quantify non-vehicular sources of PM. Among the sources unambiguously identified are construction activities, which result in elevated concentrations of coarse particulate matter (PM$_{coarse}$ = PM$_{10}$ − PM$_{2.5}$). The mobile measurements clearly highlight the spatial extent of the influence of such sources, which would otherwise be difficult to determine. Furthermore, these sources are shown to be weather-dependent, with PM$_{coarse}$ concentrations reduced by 62.1% during wet conditions compared to dry ones.

Environmental significance

Particulate matter (PM) air pollution is the leading environmental risk factor for the global burden of disease. This study provides new insights into PM sources in London, UK, through mobile monitoring that captures the spatial contributions of vehicular and non-vehicular emissions. While vehicle particulate filters are effective at reducing fine PM emissions, malfunctioning vehicles remain important contributors to urban air pollution. Additionally, construction activities are shown to be an important PM source, particularly in dry conditions, with emissions extending well beyond site boundaries. By applying novel spatial analytical techniques, this study identifies transient and stationary PM sources that must be addressed to further reduce urban PM air pollution.

1 Introduction

1.1 Background and context

Considerable progress has been made in reducing particulate matter (PM) emissions in the UK and many other parts of the world over the past three decades.[1] However, exposure to fine

[a]*Wolfson Atmospheric Chemistry Laboratories, University of York, Innovation Way, Heslington, York, YO10 5DD, UK. E-mail: sw1978@york.ac.uk*

[b]*Environmental Defense Fund, 18 Tremont Street, Boston, MA, 02108, USA*

[c]*Environmental Defense Fund Europe, 3rd Floor, 41 Eastcheap, London, EC3M 1DT, UK*

[d]*Ricardo Energy & Environment, The Gemini Building, Fermi Avenue, Harwell, OX11 0QR, UK*

† Electronic supplementary information (ESI) available. See DOI: https://doi.org/10.1039/d4em00552j

PM is the leading environmental risk factor for the global burden of disease, with emissions continuing to rise in certain regions.[2] The reduction of PM in the atmosphere remains a major challenge, and further efforts are necessary to reduce emissions and protect human health. From 1990 to 2021, UK emissions of fine particulate matter (PM$_{2.5}$) declined by 66%, and emissions of the larger size fraction of particulate matter (PM$_{10}$) decreased by 63% over the same period.[3,4] Despite this progress, the health evidence related to PM has strengthened over this period, and in September 2021, the World Health Organisation (WHO) published updated Air Quality Guidelines. The revised guideline for annual average concentrations of PM$_{2.5}$ was reduced from 10 μg m^{-3} to 5 μg m^{-3}, while the corresponding value for PM$_{10}$ was reduced from 20 μg m^{-3} to 15 μg m^{-3}.[5] These new WHO guidelines for long-term exposure to

This journal is © The Royal Society of Chemistry 2024

Environ. Sci.: Processes Impacts, 2024, **26**, 2145–2157 | 2145

pollutants reflect the lowest levels at which the guideline developers could be confident of an adverse health effect.

Meeting the WHO PM guidelines is very challenging for most countries, especially in urban areas where there are a diverse range of PM sources and high complexity associated with identifying those of the greatest importance. In 2023, the UK annual mean concentrations of $PM_{2.5}$ and PM_{10} were 7.7 μg m^{-3} and 15.2 μg m^{-3} respectively.[6] Furthermore, 79% of the UK exceeded the WHO $PM_{2.5}$ guideline, and it is estimated that in the UK over 48 000 premature deaths are attributable to $PM_{2.5}$ exposure annually.[7] The continued effort to reduce PM concentrations requires a comprehensive quantitative understanding of the contributions of different sources.

The enduring concern over PM health effects has led to a variety of emission reduction strategies, both for the precursor emissions of $PM_{2.5}$, including nitrogen oxides (NO + NO$_2$ = NO$_x$), sulfur dioxide (SO$_2$), and ammonia (NH$_3$), as well as direct reduction of primary particles. A major focus of emissions reduction has been the mitigation of PM from road transport, which has historically been a major source in urban areas. PM emissions from road transport comprise both exhaust and non-exhaust contributions. Non-exhaust PM emissions, which are becoming increasingly significant, arise from brake wear, tyre wear, road surface wear, and re-suspension of road dust, producing a variety of particle sizes, predominantly in the PM_{10} size fraction. In contrast, exhaust PM emissions originate from fuel combustion, particularly in diesel engines, producing $PM_{2.5}$ which has been the target of reduction strategies in the past two decades.

The introduction of diesel particulate filters (DPFs) for light and heavy-duty vehicles in the UK was a pivotal step to address $PM_{2.5}$ emissions from road transport. Mandated under increasingly stringent emission standards, DPFs serve as highly efficient technologies designed to physically trap particles and burn off accumulated material.[8] Following their widespread adoption in the late 2000s, DPFs have contributed largely to the 50% reduction in UK $PM_{2.5}$ emissions from road transport between 2008 and 2021.[3] Moreover, during this period of time, vehicle emission standards and control technologies have continued to develop, with gasoline vehicles in the UK requiring particulate filters from 2019 onwards, further reducing $PM_{2.5}$ emissions from road transport.[9]

As road transport emissions of PM have been reduced, the relative importance of other sources has increased. The number and type of non-vehicular sources are vast, including industrial processes, construction and demolition activities, residential heating and cooking activities.[10] $PM_{2.5}$ and PM_{10} emissions from these sources are challenging to quantify due to their transient and unpredictable nature, and there are very few primary emission factor measurements available in the literature. Efforts to mitigate PM in urban areas must encompass a broader range of sources, with a developing focus on those of non-vehicular origin.

In order to reduce $PM_{2.5}$ and PM_{10} concentrations in an urban area such as London, the concept of the *controllable fraction* of PM concentrations is important. Recent measurements of $PM_{2.5}$ show that a significant fraction originates outside the UK in the form of secondary inorganic and organic aerosol.[11] Therefore, at the city level, there is limited scope to reduce PM concentrations by controlling emissions in London itself. Nevertheless, it is important for London and other cities to quantify the PM that is locally controllable and take appropriate action to further reduce concentrations. In this respect, considering the increment in PM concentrations above the regional background provides a more meaningful metric, as it is more closely related to the controllable fraction of PM compared to absolute concentrations.

Mobile monitoring, which involves the use of fast response air quality analysers contained within a mobile laboratory, is well suited to evaluate PM emissions in urban areas, due to its ability to provide high-resolution spatial and temporal information.[12,13] Unlike stationary monitoring sites, which offer limited geographical coverage, mobile labs can traverse the urban environment measuring a diverse range of emission sources. This approach allows for the detection of transient PM emission events that might be otherwise missed, and reveals spatial patterns in PM concentrations through repeated driving routes.[14] However, working with mobile monitoring data is challenging, and new analytical techniques are required to successfully derive useful information from data with high spatial and temporal variability.

In recent research by Wilde *et al.*,[15] a new framework for analysing mobile measurements was developed. Higher NO$_x$ increments were measured in Central London compared to Outer London, and the road transport fleet-averaged emission intensity for NO$_x$ in Central London was double that of Outer London, as a consequence of high levels of dieselisation and congested traffic conditions. These findings demonstrate that the comprehensive spatial information that can be derived from mobile monitoring is essential for understanding the complex dynamics of urban air pollution, identifying emission sources, and informing targeted mitigation strategies to improve air quality.

1.2 Objectives

This study aims to use fast response mobile measurements of PM_{10} and $PM_{2.5}$, together with gaseous measurements of NO$_x$, SO$_2$ and carbon dioxide (CO$_2$), to improve understanding of PM sources in London. The main objectives are (i) to evaluate PM emissions in Central and Outer London and determine whether there is a diesel congestion penalty – elevated pollutant emissions due to the inefficient operation of emission control systems in congested traffic conditions – which has previously been observed NO$_x$ emissions in Central London; (ii) to identify and quantify the contribution made by infrequent high-emission vehicles; and (iii) to develop methods to identify and quantify non-vehicular sources of PM, considering different PM size fractions and the influence of meteorology and dispersion characteristics.

2 Data and methods

2.1 Mobile monitoring

2.1.1 Instrumentation. Mobile measurements were made using an instrumented mobile laboratory (Nissan NV400SE

2146 | *Environ. Sci.: Processes Impacts*, 2024, **26**, 2145–2157

This journal is © The Royal Society of Chemistry 2024

transit van). A detailed description of the mobile laboratory is available in the literature; a summary is provided in this text.[15,16] Air was sampled from a forward-facing inlet mounted 2.25 m above the ground at the front of the vehicle to minimise self-sampling of exhaust emissions. The risk of exhaust self-sampling is greatest when reversing and during stationary intervals. Instances where the van was reversing were excluded from the analysis, and preliminary stationary tests indicated minimal self-sampling of the exhaust, with all observed test measurements corresponding to passing vehicles.

Multiple air pollutants, including PM, NO_x, SO_2, CO_2, carbon monoxide (CO), methane (CH_4), and ozone (O_3) were measured using a variety of fast-response analysers contained within the mobile laboratory. Flame ignition tests were performed daily prior to monitoring, and instrument response times were characterised by the resulting concentration peaks.

The data from each instrument were time-aligned by calculating the optimal offset for each species using a cross-correlation procedure relative to the fastest-responding instrument. The time series for each species was shifted to produce the maximum correlation coefficient with CO_2, which was chosen as the reference measurement. A 5 s offset was applied to the data to account for the delay caused by air travelling from the sample inlet to the instruments; for typical vehicle speeds of 30–45 km h^{-1} this offset corresponds to a distance of 50 m.

Geographic location, vehicle speed, and vehicle direction were measured using a Garmin GPS 18× computer mounted externally 2.5 m above the ground. Front-facing video footage was recorded using a dashboard-mounted VANTRUE X4S 4K camera. All data were collected at 1 Hz using custom DAQFactory software, and air pollutant measurements were merged with the corresponding geographic information after the time alignment adjustments. A 'snapping' procedure was applied to correct inaccurate location measurements resulting from loss of GPS signal. Each location measurement was projected to the nearest point on a network that contained only the road links included in the mobile monitoring route. Measurements transformed more than 200 m were excluded from the analysis. This procedure was most necessary in Central London due to the high density of tall buildings near the road.

This analysis primarily considers PM, which was measured using a PALAS Air Quality Guard Ambient photometric particle number counter, which was mounted to the roof of the mobile laboratory.[17] The instrument sampled air directly and was mounted approximately 0.2 m above and 1.5 m behind the forward-facing inlet used to supply the other on-board instrumentation. Direct sampling with no sample line minimises inertial and gravitational particle losses at the instrument inlet, which are particularly relevant for larger PM size fractions. Additionally, the instrument's 360° inlet design helps to mitigate the effects of vehicle turbulence.

The instrument has a response time of 1 s and measures particles with aerodynamic diameters between 0.175 and 20 μm over 64 channels *via* single-particle optical light scattering. The mass concentrations of PM (in μg m^{-3}) are calculated for a variety of size fractions (PM_1, $PM_{2.5}$, PM_4, PM_{10}) using a mass conversion algorithm that considers the shape and duration of

the signal, and was developed alongside the EN16450 certified Fidas 200 instrument. While the PALAS Air Quality Guard Ambient offers detailed information on PM size distribution, it does not provide any data on particle composition.

Other species considered in this analysis include NO_x, CO_2, and SO_2. An Airyx Iterative Cavity-Enhanced Differential Optical Absorption Spectrometer (ICAD) was used to measure both NO_x and CO_2.[18] This instrument directly measures NO_2 in the spectral range between ≈430 and 465 nm, and an internal gas phase O_3 titration system converts NO to NO_2, allowing measurement of total NO_x. Parallel CO_2 measurements are made using a smartGAS Non-Dispersive Infra-Red (NDIR) gas sensor. In the standard configuration, this instrument has a 2 s response time; linear interpolation was applied to produce a 1 s time series.

A Thermo Model 43i Analyzer was used to measure SO_2.[19] This instrument operates on the principle of pulsed fluorescence detection and has a standard configuration with a detection limit of <1.5 μg m^{-3} and a response time of 20 s. An additional external sampling pump was employed to increase the instrument flow rate, and modifications to the software enabled 1 s measurements of SO_2. For the purposes of this study, minor changes to the detection limit resulting from these modifications are negligible, as only situations involving high SO_2 emissions (>20 μg m^{-3}) are considered.

2.1.2 Measurement location. Mobile monitoring was performed in September 2022 at two locations within London, UK (Fig. 1). Fixed driving routes were defined for each location prior to the monitoring campaign. The routes were driven continuously in alternate directions, and were designed to cover a range of road types, traffic conditions and vehicle fleet compositions, both inside and outside the Ultra Low Emission Zone (ULEZ). A summary of the driving routes at each location is provided in Table 1. The experiment was designed to contrast two areas of
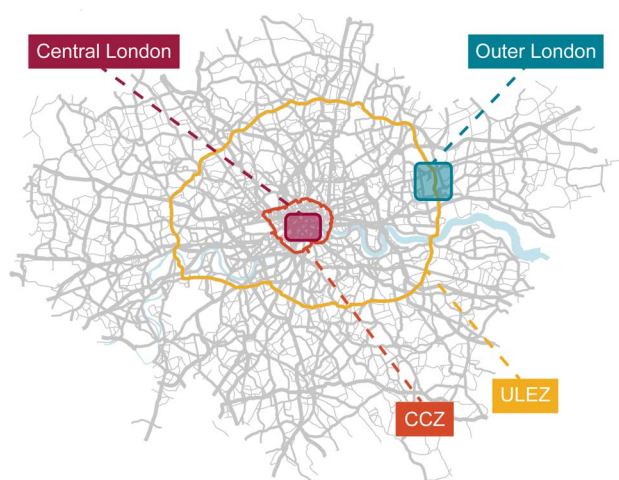

Fig. 1 Central and Outer London measurement locations. The yellow and orange lines represent the boundaries of the Ultra Low Emission Zone (ULEZ) and Congestion Charge Zone (CCZ) at the time of the monitoring campaign (September 2022), respectively. Map data courtesy of OpenStreetMap® contributors, distributed under the Open Data Commons Open Database License v1.0.

This journal is © The Royal Society of Chemistry 2024

Environ. Sci.: Processes Impacts, 2024, **26**, 2145–2157 | **2147**

Table 1 Summary information for each measurement location

Variable	Central London	Outer London
Routes completed	47	41
Route length (km)	6.2	8.0
Mean van speed (km h^{-1})	10.3	16.6
Mean temperature (°C)	25.2	24.5
Measurement start date	04 Sep	12 Sep
Measurement end date	09 Sep	15 Sep
Total raw measurements (1 Hz)	103 928	72 118

London: the highly dieselised area of Central London that suffers from congestion, and an Outer London location with a vehicle fleet more reflective of UK-wide vehicle fleet composition.

The Central London route was close to the river Thames, featured major roads, and was located within the Congestion Charge Zone (CCZ) and ULEZ. The CCZ is an area where drivers of all vehicles must pay a daily fee to reduce traffic congestion, whereas the ULEZ imposes a daily charge only on vehicles that do not meet specified stringent emission standards. The Outer London route straddled the ULEZ and featured primarily arterial and residential roads, as well as two high streets, one of which was inside the ULEZ. It should be noted that the half of the Outer London route contained within the ULEZ boundary is officially considered Inner London; for simplicity in this text, the entire route is referred to as Outer London.[20] A 2.5 km elevated section of the North Circular Road, which is a highway that surrounds London, was initially part of the Outer London route. However, since the driving conditions on this road differed significantly from those on the rest of this route and the Central London route, data from this section were excluded from the analysis.

2.2 Analysis methods

2.2.1 Background subtraction. Background subtraction isolates the local emission component of the measurements by separating the most recent, 'fresh' emissions from the urban background. The subtracted urban background concentrations represent well-mixed pollution consisting of both 'aged' local emissions, emitted long before the time of measurement, and emissions that have been transported to the measurement location from elsewhere. For a species X, once the background is subtracted, the remaining increment (ΔX) can be attributed to local emissions from nearby sources. In this work, a method described by Padilla et al. was implemented to achieve background subtraction.[21]

First, a centred 5 minute rolling window was applied to the mobile time series, which included all data 2.5 minutes before and after each 1 s measurement. Next the background concentrations for each measurement were taken as the 1st percentile value within the frame of the measurement's 5 minute window. Finally, the calculated background concentration was subtracted from the measurement value to determine the emission increment.

The 1st percentile was chosen to ensure that the smallest emission plumes were not excluded from the analysis, and sensitivity tests revealed that the choice of rolling window length did not significantly impact the calculated emission increments. Additional information about the background subtraction method can be found in the literature.[15]

2.2.2 PM size fractions. The PM component of this analysis considers the mass concentration values, in μg m^{-3}, of two particle size fractions. Fine PM (PM$_{fine}$) was defined as PM with an aerodynamic diameter less than 2.5 μm, and coarse PM (PM$_{coarse}$) was defined as PM with an aerodynamic diameter between 2.5 and 10 μm. The value of PM$_{fine}$ was taken as the PM$_{2.5}$ value reported by the PALAS Air Quality Guard instrument (eqn (1)), while PM$_{coarse}$ was calculated by subtracting this value from the reported PM$_{10}$ value (eqn (2)). Background subtraction was applied to the time series for PM$_{fine}$ and PM$_{coarse}$ after this calculation to derive the increment values ΔPM$_{fine}$ and ΔPM$_{coarse}$ (Section 2.2.1).

$$PM_{fine} = PM_{2.5} \tag{1}$$

$$PM_{coarse} = PM_{10} - PM_{2.5} \tag{2}$$

Both PM$_{fine}$ and PM$_{coarse}$ originate from a variety of sources in urban areas. Primary PM$_{fine}$ typically comes from combustion sources such as motor vehicle engines, industrial processes, and domestic/commercial activities, in particular, cooking.[22–24] The atmospheric transformation of gases such as SO$_2$ and NO$_x$ into fine particles (secondary aerosol formation) is a secondary source of urban PM$_{fine}$.[23,25] PM$_{coarse}$ is primarily emitted from abrasive mechanical sources such as motor vehicle tyre and brake wear, road dust re-suspension, and construction and demolition activities.[25–29] However, it is important to note that many of these sources emit a range of particles spanning both size fractions, and while these general descriptions are useful for data interpretation, the exact apportionment of PM$_{fine}$ and PM$_{coarse}$ to specific sources is not always possible.

Due to instrument limitations, this work does not consider ultra-fine PM with an aerodynamic diameter smaller than 0.1 μm. There is increasing evidence indicating that these particles pose significant health risks.[30] However, this analysis primarily considers PM mass concentrations, which have been shown to be largely independent of ultra-fine PM emissions due to their negligible mass, even at high particle number concentrations.[31,32] To effectively mitigate the negative health consequences of urban PM, both particle mass concentrations for PM$_{fine}$ and PM$_{coarse}$, and the particle number concentration of ultra-fine PM should be considered in combination.

2.2.3 Distance-weighted mean calculation. Distance-weighted mean concentration values were calculated using a Gaussian kernel within a continuously moving window.[15] The Gaussian kernel assigns higher weights to measurements that are closer to the data point, decreasing the weights as the distance from the point increases. The standard deviation σ, which controls the width of the Gaussian curve, influences the degree to which the measurements are weighted. This method reflects real-world concentration measurements, which are

2148 | Environ. Sci.: Processes Impacts, 2024, **26**, 2145–2157

This journal is © The Royal Society of Chemistry 2024

more strongly influenced by nearby emission sources and less by those that are distant.

This method has two main purposes: first, to provide a concentration aggregation of multiple mobile measurement circuits (47 and 41 for Central and Outer London as shown in Table 1), and second, to provide a way in which to smooth the data spatially at a predetermined scale through the choice of σ.

The driving routes in Central and Outer London were converted into networks of equally spaced 10 m points, containing 1092 and 1138 points respectively. For each species measured, mean concentrations were calculated using a two-step approach. First, the data were separated into individual complete circuits of the route and the distance-weighted mean was determined ($\sigma = 100$ m) at each 10 m point. This is similar to the drive-pass mean outlined elsewhere in the literature,[13,33] but prevents over-weighting of measurements made at locations where the mobile laboratory was moving at low speeds or stationary. Second, these values were averaged across all circuits using the arithmetic mean to determine an overall distance-weighted mean concentration for each 10 m point.

All processing was carried out using the R programming language, and the functions used to perform distance-weighted mean calculations are available in the mobilemeasr R package.[34,35] A σ value of 100 m was chosen for distance-weighted calculations to represent a near-field distance scale, over which direct exposure to urban source emissions is likely to occur.[36]

2.2.4 Non-vehicular PM source characterisation. A novel analytical method was developed to identify and quantify PM emissions from non-vehicular sources. In this work, the method is applied to two major construction sites located in Central and Outer London.

For each site, a 1 km segment of the driving route was selected, centred on the construction site. The exact midpoint of each segment represented the point on the road network closest to the geographical centre of the construction site, as identified using onboard camera data from the mobile laboratory. Next, the mobile monitoring increment measurements for both locations across all driving circuits within these 1 km segments were isolated, and the distance along the road network between each measurement and the respective construction site centre point was calculated. It is important to note that individual mobile monitoring increment concentrations (1 Hz) were used for this analysis, and not the equally spaced 10 m distance-weighted mean values discussed in Section 3.2. Generalized additive models (GAMs), which are capable of fitting non-linear relationships between variables, were then employed to evaluate the relationship between PM concentrations and the calculated distances, using the mgcv R package.[37]

The Central London data in this section of the analysis were subdivided into two categories based on the weather conditions during mobile monitoring. Onboard camera footage was used to assign each driving circuit as wet or dry, depending on the presence of precipitation and the condition of the road surface. Circuits where the weather condition changed or was unclear were omitted. All mobile monitoring in Outer London was conducted in dry weather conditions. The total number of measurements within the 1 km segments for Central London (Wet), Central London (Dry) and Outer London were 6349, 5563, and 6145 respectively.

3 Results and discussion

3.1 Central and Outer London comparison

Pollutant measurements from all driving circuits in Central and Outer London were aggregated, and the mean increments of PM_{fine}, PM_{coarse}, NO_x, CO_2 and SO_2 for each location are presented in Table 2. While these PM values represent averages, there were periods of significantly higher concentrations of PM_{fine} and PM_{coarse} within the data set. Specifically, the maximum increments of PM_{fine} reached 92.0 µg m^{-3} in Central London and 271.8 µg m^{-3} in Outer London, whereas PM_{coarse} peaked at 207.8 µg m^{-3} in Central London and 221.7 µg m^{-3} in Outer London. These episodic peaks in PM are important as they increase short-term human exposure, potentially leading to acute health effects.

A direct comparison of these values and those in Table 2 with WHO guidelines is not appropriate, as the reported values are concentration increments rather than absolute concentrations. However, these increments represent the controllable fraction of PM, which is critical for informing future PM reduction strategies for London. A limitation of this study is a lack of PM composition information, which, if available, would enable a more in-depth apportionment of the measured PM increments to different urban sources, such as road transport (exhaust and non-exhaust), industrial processes, and domestic/commercial activities. Previous research indicates that PM in urban areas has traditionally been dominated by road transport emissions; however, recent studies have highlighted the importance of other non-vehicular sources, including commercial and domestic cooking, as well as construction activities.[22–24,28,38] The focus of this section, road transport PM emissions, are generally controlled by three main factors: total traffic volume, traffic congestion, and vehicle fleet composition.

Combustion is the primary source of CO_2 in urban environments, with vehicle exhaust emissions as the main contributor.[39] Therefore, the mean ΔCO_2 concentrations likely

Table 2 Mean increment concentrations of PM_{fine}, PM_{coarse}, NO_x, CO_2, and SO_2 at each measurement location, presented with 95% confidence intervals. Mean values were calculated from all 1 Hz increment measurements at each location. 95% confidence intervals were calculated using the standard error of the mean and a z-score = 1.96. Percentage differences were calculated relative to the Outer London data

Species	Concentration (µg m^{-3})		% Difference
	Central London	Outer London	
ΔPM_{fine}	2.83 ± 0.02	3.62 ± 0.05	−21.9
ΔPM_{coarse}	5.93 ± 0.05	5.35 ± 0.05	+10.8
ΔNO_x	175.8 ± 1.8	101.9 ± 1.6	+72.5
ΔCO_2 (×10^3)	51.0 ± 0.3	45.0 ± 0.3	+13.4
ΔSO_2	2.72 ± 0.01	3.04 ± 0.07	−10.5

This journal is © The Royal Society of Chemistry 2024

Environ. Sci.: Processes Impacts, 2024, **26**, 2145–2157 | **2149**

reflect vehicle combustion activity, suggesting that total traffic volume was slightly higher in Central London compared to Outer London. This is supported by the mean ΔPM_{coarse} concentration, which was 10.8% higher in Central London, aligning with the 13.4% difference in ΔCO_2 values. PM_{coarse} in urban areas can be largely attributed to non-exhaust vehicle emissions such as tyre and brake wear, road surface wear, and dust re-suspension, and therefore also act as a tracer species for total traffic volume.[28] It is important to note that the emissions of CO_2 and PM_{coarse} are not entirely independent of traffic congestion and vehicle fleet composition, and the differences in these variables between locations will influence the results. However, total traffic volume is still likely to dominate the trends observed in mean increment concentrations.

In contrast, both NO_x and PM_{fine} emissions are considerably more sensitive to vehicle fleet composition, due to the variability of the emission control systems fitted to vehicles of different types and ages. NO_x emissions are also highly sensitive to traffic congestion because of the complexity of the emissions control systems that reduce NO_x. Typically, exhaust NO_x from diesel vehicles – the highest NO_x emitters – is controlled using selective catalytic reduction (SCR) or a lean NO_x trap (LNT); both operate on the principle of chemical reduction and are highly dependent on the operating parameters of the engine and traffic conditions.[8] Exhaust PM, which consists mainly of PM_{fine}, is controlled using particulate filters that physically trap particles and burn off accumulated material.[8]

Differences in traffic congestion and vehicle fleet composition at each measurement location arise from the nature and position of the chosen driving routes and explain the observed NO_x and PM_{fine} increment concentrations. The Central London measurement location was a busy urban centre inside the CCZ and ULEZ, and so the vehicle fleet was comprised mostly of newer vehicles conforming to the most stringent emission standards. However, traffic flow was poor and congestion was frequent, as evidenced by the mean van speed shown in Table 1. In contrast, the Outer London measurement location was partially outside of the ULEZ, with approximately half of the driving route extending beyond the boundary. This portion of the route included older vehicles, with greater wear and less effective or deteriorated emission control systems (Section 3.3). However, traffic at the Outer London location was more free-flowing than in Central London, and congestion was less frequent, resulting in an increase of over 60% in the mean speed of the van at this location (see Table 1).

The ΔNO_x concentrations presented in Table 2 are likely dominated by the impact of traffic congestion; the mean in Central London was 72.5% higher than in Outer London. This increase is consistent with the results reported by Wilde et al.[15] and can be attributed to the congestion penalty associated with the inefficient operation of SCR and LNT emission control systems. Conversely, the mean ΔPM_{fine} concentration in Central London was 21.9% lower than in Outer London. This result is important, indicating that there is no congestion penalty for PM_{fine} in Central London and that concentrations are predominantly influenced by the composition of the vehicle fleet. Furthermore, unlike NO_x emission control systems, these

data provide evidence for the success of particulate filters, which remain efficient even under congested conditions.

However, it is still important to acknowledge the impact of vehicle fleet composition on PM_{fine} emissions. The higher mean ΔPM_{fine} concentration in Outer London can be attributed to the non-ULEZ portion of the driving route, which includes non-ULEZ compliant vehicles. Many of these older vehicles are not fitted with particulate filters, and those that are have accumulated wear reducing their effectiveness. Moreover, as vehicles age, they can develop engine faults that increase pollutant emissions, which, when coupled with the lack of an effective emission control system, may contribute to the episodic high concentration peaks contained within the mobile monitoring data.

To quantify the effects of the ULEZ and vehicle fleet composition, mobile monitoring data from Outer London were split into two groups: measurements taken inside the ULEZ ($n =$ 43 957) and outside the ULEZ ($n =$ 28 161). Mean pollutant increments for each group were recalculated and are presented in Table S1 of the ESI.† The mean δPM_{fine} concentration was 38.4% higher outside the ULEZ than inside, while the mean δPM_{coarse} concentration was 6.6% lower. This substantial difference in δPM_{fine} highlights the strong impact of the ULEZ and vehicle fleet composition on urban PM_{fine} emissions. A comparison of mean δPM_{fine} and δNO_x concentrations for the inside ULEZ data for Outer London with the Central London data (which was collected entirely within the ULEZ) showed increases of 14.9% and 63.1% respectively. The relatively small increase in δPM_{fine}, consistent with the δCO_2 increase of 17.2% for the same comparison, supports the absence of a congestion penalty for PM_{fine}. For δNO_x in Outer London, the mean concentration was 14.0% lower outside the ULEZ than inside, suggesting that while vehicle fleet composition is a dominant factor in urban PM_{fine} emissions, it has less impact on NO_x emissions.

To further reduce PM_{fine} in Outer London and more widely, it is critical to consider ageing and deteriorated vehicles, especially those with exceptionally high emissions. The mean ΔSO_2 concentration for Central London was 10.5% lower than that of Outer London. This difference can be explained by a single high-emission vehicle event and is explored further in Section 3.3.

3.2 Distance-weighted PM concentrations

A key feature of mobile monitoring is the spatial information it can provide. Distance-weighted mean concentrations of ΔPM_{fine} and ΔPM_{coarse} were calculated for 10 m points along each driving circuit in Central and Outer London, and the values at each point across all driving circuits were aggregated. A statistical summary of these data is provided in Table 3, and Fig. 2 presents a spatial distribution for each PM size fraction at each measurement location.

The results in Table 3 differ from those in Table 2 in that they were calculated from the mobile data after 10 m distance-weighted aggregation. The statistics presented in Table 3 therefore reflect the distribution of the distance-weighted spatial averages, and not the raw measurements. Although the

2150 | Environ. Sci.: Processes Impacts, 2024, 26, 2145–2157

This journal is © The Royal Society of Chemistry 2024

Table 3 Statistical summary of distance-weighted increment concentrations at each equally spaced 10 m point in Central and Outer London. The values represent the arithmetic mean of the distance-weighted increments calculated for each 10 m point, across all driving routes. Sample sizes are $n = 1092$ for Central London and $n = 1138$ for Outer London

Species	Mean	Min	Q25	Med	Q75	Max
Central London ($\mu g\ m^{-3}$)						
ΔPM_{fine}	2.74	1.43	2.56	2.74	2.89	4.78
ΔPM_{coarse}	5.74	2.34	5.10	5.69	6.14	11.29
Outer London ($\mu g\ m^{-3}$)						
ΔPM_{fine}	3.65	1.46	2.73	3.45	4.42	15.57
ΔPM_{coarse}	5.27	1.27	4.53	5.34	5.93	10.33

mean values of ΔPM_{fine} and ΔPM_{coarse} in Table 3 for each location follow the same trends as discussed in Section 3.1, their exact values are not identical to those in Table 2 because they are influenced by the spatial variability of the mobile measurements.

The magnitude of the difference between ΔPM_{fine} for Outer and Central London increases when moving from the minimum (2.0%) through the 25th quantile (2.9%), median (6.2%), 75th quantile (34.6%), to the maximum (69.3%). This trend is visualised in Fig. S1 of the ESI† and shows that the difference in ΔPM_{fine} between locations is heavily biased toward the upper end of the measured distribution, likely due to aged and deteriorated vehicles within the on-road fleet.
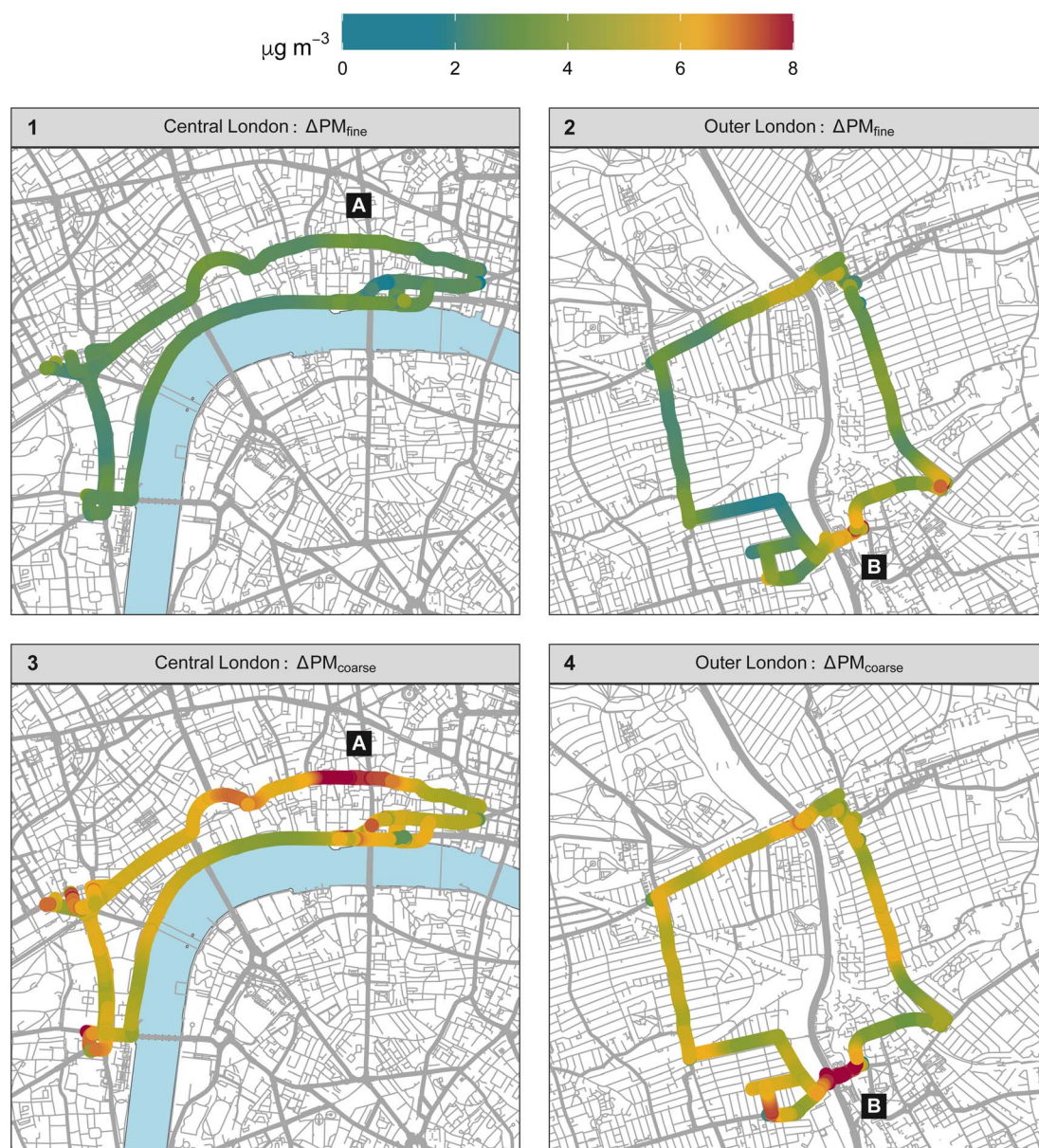
Fig. 2 Spatial distributions of the distance-weighted mean concentrations of PM_{fine} (panels 1 and 2) and PM_{coarse} (panels 3 and 4) in Central and Outer London. A and B denote the positions of major construction sites in Central and Outer London respectively. Map data courtesy of OpenStreetMap® contributors, distributed under the Open Data Commons Open Database License v1.0.

This journal is © The Royal Society of Chemistry 2024

Environ. Sci.: Processes Impacts, 2024, **26**, 2145–2157 | **2151**

The four panels in Fig. 2 visually show the trends discussed in PM concentrations, as well as additional variation along driving routes, with elevations near busy intersections with increased traffic. These features of the spatial distributions, particularly for δPM_{fine}, suggest that most measurements along each route were dominated by road traffic emissions rather than other sources. If sources such as industrial activities or residential and commercial cooking had consistently contributed to the measurements, the spatial distributions in Fig. 2 would likely display localized enhancements corresponding to their locations. Panel 2 of Fig. 2 shows elevated ΔPM_{fine} concentrations around an area of the road that contained an individual high-emission vehicle (Fig. S4 in the ESI†). This transient event, which occurred on a single driving circuit, produced ΔPM_{fine} concentrations high enough to influence the average aggregate values across all 47 circuits in Outer London, and is discussed in more detail in Section 3.3.

Labels A and B in Fig. 2 indicate two areas of highly elevated concentrations of ΔPM_{fine} and ΔPM_{coarse}, with an emphasis on the latter. The increased concentrations at locations A and B were consistent across all driving circuits and therefore could not be attributed to transient one-off events. Inspection of the mobile laboratory's onboard camera footage revealed positions A and B corresponded exactly with major construction sites in Central and Outer London. Construction sites A and B featured non-road mobile machinery and extended 78 m and 104 m, respectively, alongside the driving route at each location. Images of these sites can be found in Fig. S2 of the ESI.† The mean concentrations of raw ΔPM_{coarse} measurements within 100 m of the centre points of A and B were 9.56 µg m^{-3} and 6.42 µg m^{-3} respectively, 66.6% and 21.8% higher than the overall location mean values reported in Table 3. It should be noted that in Outer London, the section of road containing an individual high-emission vehicle overlapped with the position of construction site B (Section 3.3). However, the ΔPM_{coarse} contribution from the high-emission vehicle was relatively low (Fig. 3), and insufficient to explain the observed increase. Many of the data points within 100 m of the construction sites populated the upper end of the distance-weighted concentration increment distributions for both measurement locations and PM size fractions, as shown in Fig. S1 in the ESI.† The reported results provide evidence for the increasing importance of non-vehicular PM sources amidst the successful control of vehicle emissions, which is discussed further in Section 3.4.

3.3 High-emission vehicles

Mobile monitoring data from Outer London demonstrate the substantial impact that individual high-emission vehicles can have on PM concentrations. While measuring in the non-ULEZ section of the driving route, a car emitting visible blue/white smoke from its exhaust joined the road two vehicles ahead of the mobile laboratory. This vehicle was tracked for 1.2 km, and the resulting concentration increments of PM_{fine}, PM_{coarse}, and SO_2 during this period are shown in Fig. 3. A photograph of the high-emission vehicle and a map illustrating the section of the driving route on which it was measured are provided in Fig. S3 (photo 1) and S4 of the ESI.†

During the approximately 10 minute period following the high-emission vehicle, elevated concentrations of PM_{fine} were observed, with frequent peaks ranging from 100 to 200 µg m^{-3}, corresponding to the vehicle's acceleration at traffic lights and roundabouts. The average measured ΔPM_{fine} concentration while tracking the vehicle was 51.27 µg m^{-3}, more than 17 times higher than average for the rest of the measurements on the same driving circuit (3.00 µg m^{-3}). Moreover, despite occurring only on a section of a single driving circuit, the impact of the high-emission vehicle is visible in the spatial distribution of distance-weighted mean concentrations presented in panel 2 of Fig. 2.

In addition to identifying high PM emissions from individual vehicles, mobile monitoring provides multi-pollutant information. The co-emission of SO_2 (shown in Fig. 3) is indicative of an engine malfunction resulting in lubricant combustion. Outside of this high-emission event, measured SO_2 increment concentrations were consistently low with mean values of 2.5 and 2.7 µg m^{-3} in Central and Outer London respectively. These results are expected given vehicle fuel in the UK is regulated and must have a sulfur content lower than 10 ppm.[40] Engine lubricant, however, often contains sulfur in greater quantities to improve anti-wear properties.[41,42] Although this lubricant is not designed to be burnt in a vehicle's engine, deterioration or malfunction can result in combustion of the lubricant, and subsequent elevated emission of both SO_2 and PM through a variety of mechanisms.[42–44]

The registration number of the high-emission vehicle was captured by the onboard camera of the mobile laboratory and cross-referenced with the Driver and Vehicle Licensing Agency (DVLA) vehicle database to access its technical specifications and vehicle safety inspection information.[45] Registered in 2006, the Euro 4 gasoline car had covered approximately 116 000 miles at its safety inspection in January 2023, 4 months after the mobile monitoring campaign. This vehicle model was not fitted with a particulate filter, which, when combined with lubricant
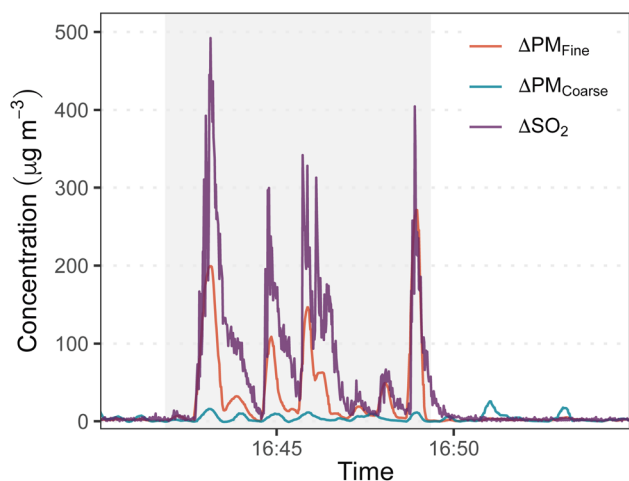

Fig. 3 Time series tracking a high emission vehicle in Outer London. The grey shaded area represents the time period during which the vehicle was being measured.

2152 | Environ. Sci.: Processes Impacts, 2024, 26, 2145–2157

This journal is © The Royal Society of Chemistry 2024

combustion which increases PM emission, explains the measured ΔPM_{fine} concentrations. Furthermore, the vehicle failed the aforementioned safety inspection due to a warning light indicating an engine malfunction, and additional notes from the inspection state that blue smoke was emitted during acceleration.[45]

Filtering the mobile monitoring data ΔPM_{fine} and ΔSO_2 to include only values above the 99th percentile (11.90 and 9.41 µg m^{-3} respectively) revealed a second high-emission vehicle, which was measured during a transit period within Outer London, outside of the designated measurement route (ESI Fig. S3† photo 2). The mobile laboratory tracked behind this vehicle on a road outside of the ULEZ for 0.5 km over a 2 minute period. The resulting increment concentrations of up to 50 µg m^{-3} for PM_{fine} and SO_2, as well as those for PM_{coarse} are presented in Fig. S5 in the ESI.† This vehicle was a 2007 Euro 4 gasoline car without a particulate filter, and the co-emission of SO_2 and PM_{fine} suggest engine malfunction and subsequent lubricant combustion. As the vehicle was not measured on the specified driving route, it was not included in the primary analysis.

Although the two high-emission vehicles observed during this study represent outliers in terms of their malfunctioning status and associated PM_{fine} emissions, their potential contribution to overall fleet emissions is significant. The high-emission vehicle measured on the driving route was present for less than 0.15% of the total distance driven in Outer London; however, its presence increased the overall mean ΔPM_{fine} concentration (shown in Table 2) by 7.4%. The mean increment concentrations in Outer London with the high-emission vehicle removed are provided in Table S2 of the ESI.† Previous research using a range of stationary measurement techniques report that high-emission vehicles representing a small fraction of the total vehicle fleet are responsible for a disproportionate share of total PM emissions, particularly for gasoline vehicles.[46,47] The results of this study agree with these findings, and demonstrate the suitability of mobile monitoring for the detection, quantification, and explanation of high-emission vehicles, which must be targeted to effectively control PM in urban areas.

3.4 Non-vehicular PM sources

To further characterise and quantify PM emissions from construction sites A and B, a 1 km segment of the driving route at each location was isolated, centred on the respective site. The PM increment measurements within each segment were used in combination with GAMs to calculate the average concentrations of ΔPM_{fine} and ΔPM_{coarse} as a function of the distance from the construction site. In Outer London, measurements that corresponded with the nearby high-emission vehicle comprised 4.7% of the data, and were excluded from this part of the analysis to ensure that influence of construction site B on ΔPM_{fine} could be better evaluated. The data from Central London were divided into two categories, 'Wet' or 'Dry', based on weather condition; the results for these two categories and those for Outer London, where the weather condition was always dry, are presented in Fig. 4.

Panel 2 in Fig. 4 shows a clear Gaussian peak centred on construction site A, with concentrations of ΔPM_{fine} and ΔPM_{coarse} reaching maximum values of 5.21 µg m^{-3} and 22.50 µg m^{-3} respectively. Both ΔPM_{fine} and ΔPM_{coarse} concentrations rapidly decayed with increasing distance from the origin in both directions. The two smaller peaks adjacent to the primary peak associated with construction site A could be attributed to other minor construction activities within the 1 km road segment; this was confirmed by footage from the on-board camera (Fig. S6 in the ESI†). These minor construction activities did not contain non-road mobile machinery and extended much smaller distances along the driving route (25 m and 15 m). The peaks associated with these activities were not obvious when examining the spatial distributions of overall PM increments in Section 2.2.3, however they became apparent when using a more targeted analytical approach.

The footage from the onboard camera was reviewed to identify other possible (false-negative) construction activities that were not apparent in the mobile monitoring data. There were no other major construction activities (containing non-road mobile machinery and extending more than 50 m along the driving route), highlighting the effectiveness of distance-weighted mobile monitoring techniques for detecting large non-transient non-vehicular PM sources. There were 4 and 2 additional minor construction activities identified in Central and Outer London respectively. Similar to the minor construction activities presented in Fig. 4, these sites were not obvious in the overall spatial distribution data. Repeating the same targeted analytical approach that was used to investigate construction sites A and B, but with a 250 m segment of road centred on each minor construction site, revealed that each activity was associated with a concentration peak of ΔPM_{fine} and ΔPM_{coarse}, with maximum values ranging between 2.48–5.19 µg m^{-3} and 6.25–15.76 µg m^{-3} respectively. As well as further demonstrating the utility of combining mobile measurements with a targeted analytical approach, these results highlight the benefit of recording camera footage when performing mobile monitoring.

Comparison of PM increment distributions for the different meteorological conditions in Central London (Fig. 4: panel 1 and 2) revealed that wet weather was correlated with a reduction in PM emissions from construction site A. This effect was particularly prominent for PM_{coarse}, with the peak increment concentration reduced by 62.1%. The exact reason for this observation could not be determined conclusively and was likely the result of a combination of factors. Precipitation has been shown to reduce PM concentrations through scavenging and wet deposition, and wet road conditions can decrease the mobility of settled PM, suppressing emissions from re-suspension.[48,49] It is also possible that the observed decline in PM was attributable to a reduction in construction activity, arising from unfavourable wet weather conditions that made outdoor work difficult.

Although meteorological variations in Central London significantly impacted PM levels near construction site A, their effect on the rest of the driving route was much smaller. Table S1 in the ESI† presents the average concentrations of PM
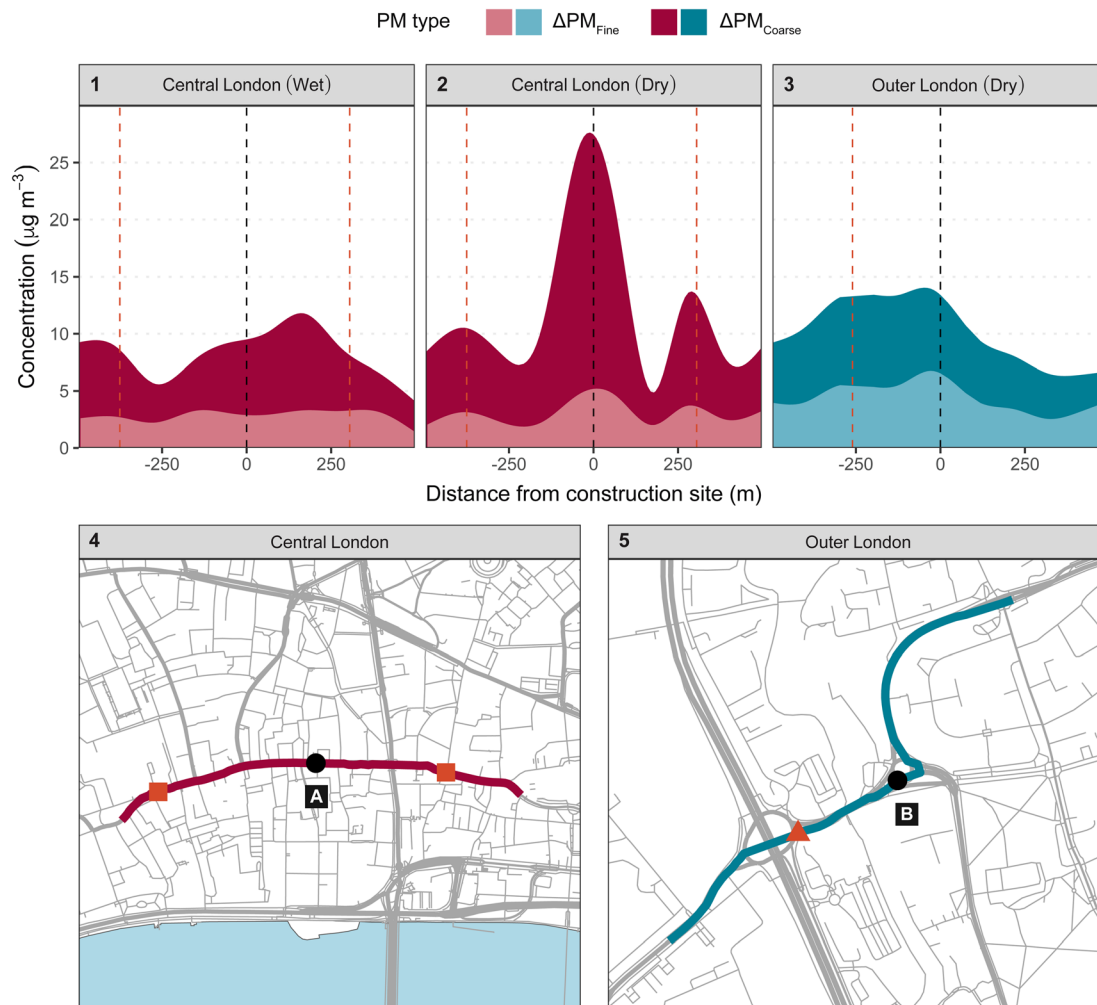
This journal is © The Royal Society of Chemistry 2024

Environ. Sci.: Processes Impacts, 2024, **26**, 2145–2157 | **2153**

Fig. 4 Concentrations of ΔPM_{fine} and ΔPM_{coarse} within a 1 km road segment centred on major construction sites A and B in Central and Outer London respectively, calculated using GAMs. Panels 1, 2, and 3 show PM mass concentration as a function of distance from the construction site, with PM_{coarse} concentrations stacked on PM_{fine} concentrations. The Central London data are separated into wet and dry weather conditions, all measurements for Outer London were made in dry conditions. Panels 4 and 5 show spatially the respective 1 km road segment for each site. The two orange dashed lines and orange squares in panels 1, 2, and 4 denote the position of smaller secondary construction work in Central London. The orange dashed line and triangle in panels 3 and 5 denote the position of a large multi-lane roundabout in Outer London. Map data courtesy of OpenStreetMap® contributors, distributed under the Open Data Commons Open Database License v1.0.

increments under each meteorological condition for the entire Central London driving route, excluding measurements within 100 m of the construction site A. There was a 13.8% difference in increments of PM_{fine} and a 15.2% difference in increments of PM_{coarse} between wet and dry conditions. Additionally, when comparing the dry Central London data with the Outer London data, all previously discussed trends and observations remained consistent.

The influence of construction site B on the Outer London observations in Fig. 4 was less obvious than the influence of construction site A on the dry Central London observations, despite similar weather conditions. This difference was likely the result of variation in the types of construction activities on sites A and B, as well as differences in the surrounding urban environment. The maximum concentrations of ΔPM_{fine} and ΔPM_{coarse} around the construction site in Outer London were 6.76 µg m^{-3} and 8.07 µg m^{-3} respectively, much lower than

those around the construction site in Central London during dry weather. Furthermore, the relative contributions from each PM size fraction at the maximum were different, with PM_{fine} accounting for only 19.1% of total PM (PM_{fine} + PM_{coarse}) in dry Central London, but accounting for 45.6% of total PM in Outer London. This observation may have been a result of increased combustion activity producing more PM_{fine} at construction site B when compared to site A, however, no correlation was observed between PM and gaseous combustion species such as CO_2 or NO_x. It is more likely that within the increments of PM_{fine} in Outer London, there was a greater contribution from road transport vehicles compared to Central London, for the reasons outlined previously in the text (Section 3.1). Furthermore, there was a large multi-lane roundabout located 250 m from construction site B, as highlighted in panels 3 and 5 of Fig. 4. The heavy traffic and congestion on this part of the driving route was likely responsible for the additional PM peak

2154 | *Environ. Sci.: Processes Impacts*, 2024, **26**, 2145–2157

This journal is © The Royal Society of Chemistry 2024

in Outer London, arising from a mix of primary vehicle exhaust and non-exhaust emissions, as well as re-suspended particles from construction activities at the nearby site B. No elevated ΔSO_2 concentrations were observed at either construction site.

In addition to local meteorological conditions, other aspects of the mobile monitoring data can help to further characterise non-vehicular PM sources, such as considering the driving direction in dry Central London. This specific location and meteorological condition were chosen for further analysis due to the distinct peak observed for construction site A, and the fact that there was minimal interference from the surrounding urban environment. Mobile measurements were then grouped by the direction that the mobile laboratory was travelling around the driving route (clockwise or anticlockwise). Vehicles in the UK drive on the left-hand side of the road, and so measurements from the anticlockwise driving route will be closer to construction site A than those from the clockwise driving route. Fig. S7 in the ESI† presents the concentrations of PM increments in dry Central London, separated by the direction of travel of the mobile lab, and therefore the distance relative to construction site A.

The maximum average ΔPM_{fine} and ΔPM_{coarse} values were 64.3% and 81.9% higher, respectively, when travelling on the side of the road closest to the construction site compared to maximum values on the side of the road further away. Moreover, comparing the lower bound of the 95% confidence interval for the closer side of the road to the upper bound for the further side, the absolute difference in maximum ΔPM_{fine} and ΔPM_{coarse} values were 1.81 μg m^{-3} and 8.62 μg m^{-3} respectively, highlighting the statistical significance of the observed differences. The decrease in ΔPM_{coarse} across the road is strongly indicative of a local source where concentration gradients change dramatically over short distances. Similarly to the along-road fall-off in concentration of ΔPM_{coarse} (shown in Fig. 4), the perpendicular decrease across the road in ΔPM_{coarse} concentration is also strong. The stronger concentration gradients observed for ΔPM_{coarse} compared to ΔPM_{fine} are expected, as larger particles have greater mass and are more susceptible to gravitational settling, limiting their transport distance from the source.

These results highlight a distinct advantage of performing the mobile monitoring driving routes in both directions. Measuring across the full width of the carriageway ensures that proximate non-vehicular emission sources on both sides of the road are included in the measurements, and enables the gradient of their fall-off in concentration to be quantified. Furthermore, driving in both directions provides a more accurate representation of the spatial variability of emissions along the road network, especially at junctions, where traffic conditions upon approach are often different from those after exit.

The identification, quantification, and characterisation of construction sites A and B were only possible due to the unique information provided by mobile monitoring. Moreover, the campaign from which the data were obtained was not originally designed to target non-vehicular PM sources; their discovery was possible through robust spatial analysis of the mobile measurements and subsequent development of novel techniques. Furthermore, the developed techniques can be easily extended to investigate non-vehicular PM sources in various locations and from different origins. For instance, cooking emissions from restaurants have recently been identified as a significant contributor to urban PM$_{fine}$ concentrations.[24,38] This study highlights the increasing importance of non-vehicular sources in urban areas amidst the successful control of vehicular PM emissions, and provides a foundation upon which to develop future research and inform mitigation strategies.

4 Conclusions

Fast-response mobile measurements provide excellent opportunities to understand the nature of emission sources in urban environments. However, they introduce complexities for data analysis because they vary in both space and time. Nevertheless, this work demonstrates robust strategies that can be adopted to maximise the insights that can be obtained from such measurements. First, the repeated measurement of road links (in this study approximately 50) in both traffic directions maximises the opportunity to detect 'persistent' rather than transient sources. Second, simultaneous measurement of multiple pollutants greatly improves the ability to link concentration measurements with specific types of emission sources. In this study, SO$_2$ was shown to be a key tracer compound that can be used to identify the few high-sulfur combustion emission sources remaining in a city such as London. Similarly, the measurement of both PM$_{fine}$ and PM$_{coarse}$ enables non-combustion sources of PM to be unambiguously identified.

As historically dominant sources of PM in urban areas, such as road vehicle exhaust emissions, continue to decline, the need to better understand and quantify various poorly characterised sources, such as construction activities and individual high-emission vehicles, becomes increasingly important. Often, these sources are transient in nature or have an uncertain spatial distribution, making it difficult to evaluate their impact using fixed-site measurements. Mobile monitoring offers a dynamic approach to address these challenges. As PM measurement techniques advance, the ability to obtain highly disaggregated measurements of particle composition will further assist in this goal.

Data availability

All data for this article, including mobile monitoring increment data and example analysis scripts, are available at **https://www.github.com/thesamwilson/mobile_monitoring_data_availability**. The mobilemeasr R package can be found at **https://www.github.com/shonawilde/mobilemeasr**.

Author contributions

Samuel Wilson: methodology, validation, formal analysis, investigation, data curation, visualization, writing—original

This journal is © The Royal Society of Chemistry 2024

Environ. Sci.: Processes Impacts, 2024, **26**, 2145–2157 | **2155**

Conflicts of interest

There are no conflicts to declare.

Acknowledgements

References

1 M. S. Hammer, A. van Donkelaar, C. Li, A. Lyapustin, A. M. Sayer, N. C. Hsu, R. C. Levy, M. J. Garay, O. V. Kalashnikova, R. A. Kahn, et al., Environ. Sci. Technol., 2020, 54, 7879–7890.

2 Z. Klimont, K. Kupiainen, C. Heyes, P. Purohit, J. Cofala, P. Rafaj, J. Borken-Kleefeld and W. Schöpp, Atmos. Chem. Phys., 2017, 17, 8681–8723.

3 UK National Atmospheric Emissions Inventory, Pollutant Information: PM₁₀, 2021, https://www.naei.beis.gov.uk/overview/pollutants?pollutant_id=122, accessed 17 May 2024.

4 UK National Atmospheric Emissions Inventory, Pollutant Information: PM₂.₅, 2021, https://www.naei.beis.gov.uk/overview/pollutants?pollutant_id=24, accessed 17 May 2024.

5 World Health Organization, WHO global air quality guidelines: particulate matter (PM2.5 and PM10), ozone, nitrogen dioxide, sulfur dioxide and carbon monoxide, 2021, https://www.who.int/publications/i/item/9789240034228, accessed 17 May 2024.

6 Department for Environment Food & Rural Affairs, National Statistics: Particulate Matter, 2024, https://www.gov.uk/government/statistics/air-quality-statistics/concentrations-of-particulate-matter-pm10-and-pm25#trends-in-concentrations-of-pm10-in-the-uk-1992-to-2023, accessed 17 May 2024.

7 E. A. Marais, J. M. Kelly, K. Vohra, Y. Li, G. Lu, N. Hina and E. C. Rowe, GeoHealth, 2023, 7, e2023GH000910.

8 M. V. Twigg, Philos. Trans. R. Soc., A, 2005, 363, 1013–1033.

9 B. Giechaskiel, A. Joshi, L. Ntziachristos and P. Dilara, Catalysts, 2019, 9, 586.

10 R. M. Harrison, Philos. Trans. R. Soc., A, 2020, 378, 20190319.

11 P. Monks, D. Carruthers, D. Carslaw, C. Dore, R. Harrison, M. Heal, M. Jenkin, A. Lewis, J. Stedman and A. Tomlin, et al., Mitigation of United Kingdom PM₂.₅ Concentrations, AQEG, 2015.

12 L. E. Cummings, J. D. Stewart, R. Reist, K. M. Shakya and P. Kremer, Front. Built Environ., 2021, 7, 648620.

13 J. S. Apte, K. P. Messier, S. Gani, M. Brauer, T. W. Kirchstetter, M. M. Lunden, J. D. Marshall, C. J. Portier, R. C. Vermeulen and S. P. Hamburg, Environ. Sci. Technol., 2017, 51, 6999–7008.

14 S. Hu, S. E. Paulson, S. Fruin, K. Kozawa, S. Mara and A. M. Winer, Atmos. Environ., 2012, 51, 311–319.

15 S. E. Wilde, L. E. Padilla, N. J. Farren, R. A. Alvarez, S. Wilson, J. D. Lee, R. L. Wagner, G. Slater, D. Peters and D. C. Carslaw, Atmos. Environ.: X, 2024, 21, 100241.

16 R. L. Wagner, N. J. Farren, J. Davison, S. Young, J. R. Hopkins, A. C. Lewis, D. C. Carslaw and M. D. Shaw, Atmos. Meas. Tech., 2021, 14, 6083–6100.

17 PALAS, AQ Guard System Information, 2024, https://www.palas.de/en/product/aq-guard?save=accept, accessed 24 April 2023.

18 Airyx, ICAD in situ NOx monitor, 2024, https://www.airyx.de/item/icad/, accessed 24 April 2023.

19 Thermo Fischer Scientific, Model 43i SO2 analyzer, 2024, https://www.thermofisher.com/order/catalog/product/43I, accessed 24 April 2023.

20 The London Plan 2021, Annex 2 – Inner and Outer London Boroughs, 2021, https://www.london.gov.uk/programmes-strategies/planning/london-plan/the-london-plan-2021-online/annex-2-inner-and-outer-london-boroughs, accessed 17 May 2023.

21 L. E. Padilla, G. Q. Ma, D. Peters, M. Dupuy-Todd, E. Forsyth, A. Stidworthy, J. Mills, S. Bell, I. Hayward, G. Coppin, et al., Atmos. Environ., 2022, 270, 118851.

22 F. Karagulian, C. A. Belis, C. F. C. Dora, A. M. Prüss-Ustün, S. Bonjour, H. Adair-Rohani and M. Amann, Atmos. Environ., 2015, 120, 475–483.

23 M. Elser, C. Bozzetti, I. El-Haddad, M. Maasikmets, E. Teinemaa, R. Richter, R. Wolf, J. G. Slowik, U. Baltensperger and A. S. Prévôt, Atmos. Chem. Phys., 2016, 16, 7117–7134.

24 P. K. Saha, A. A. Presto, S. Hankey, B. N. Murphy, C. Allen, W. Zhang, J. D. Marshall and A. L. Robinson, Environ. Sci. Technol., 2022, 56, 14284–14295.

25 R. M. Harrison, A. R. Deacon, M. R. Jones and R. S. Appleby, Atmos. Environ., 1997, 31, 4103–4117.

26 K. M. Latha and E. Highwood, J. Quant. Spectrosc. Radiat. Transfer, 2006, 101, 367–379.

27 D. Jandacka and D. Durcanska, Atmosphere, 2019, 10, 583.

2156 | Environ. Sci.: Processes Impacts, 2024, 26, 2145–2157

This journal is © The Royal Society of Chemistry 2024

28 V. N. Matthaios, J. Lawrence, M. A. Martins, S. T. Ferguson, J. M. Wolfson, R. M. Harrison and P. Koutrakis, *Sci. Total Environ.*, 2022, **835**, 155368.

29 A. Font, T. Baker, I. S. Mudway, E. Purdie, C. Dunster and G. W. Fuller, *Sci. Total Environ.*, 2014, **497**, 123–132.

30 D. E. Schraufnagel, *Exp. Mol. Med.*, 2020, **52**, 311–317.

31 R. M. Harrison, J. P. Shi, S. Xi, A. Khan, D. Mark, R. Kinnersley and J. Yin, *Philos. Trans. R. Soc., A*, 2000, **358**, 2567–2580.

32 P. Kumar, A. Robins, S. Vardoulakis and R. Britter, *Atmos. Environ.*, 2010, **44**, 5035–5052.

33 D. J. Miller, B. Actkinson, L. Padilla, R. J. Griffin, K. Moore, P. G. T. Lewis, R. Gardner-Frolick, E. Craft, C. J. Portier, S. P. Hamburg, *et al.*, *Environ. Sci. Technol.*, 2020, **54**, 2133–2142.

34 R Core Team, *R: A Language and Environment for Statistical Computing*, R Foundation for Statistical Computing, 2013.

35 S. Wilde, *mobilemeasr: Tools to Perform Data Analysis on Mobile Measurements*, 2022.

36 A. Y. Watson, R. R. Bates and D. Kennedy, *Atmospheric Transport and Dispersion of Air Pollutants Associated with Vehicular Emissions*, National Academies Press (US), 1988.

37 S. N. Wood, *mgcv: Mixed GAM Computation Vehicle with Automatic Smoothness Estimation*, 2017.

38 R. Song, A. A. Presto, P. Saha, N. Zimmerman, A. Ellis and R. Subramanian, *Air Qual., Atmos. Health*, 2021, **14**, 2059–2072.

39 Department for Transport, *Transport and environment statistics: 2023*, 2023, https://www.gov.uk/government/statistics/transport-and-environment-statistics-2023/transport-and-environment-statistics-2023, accessed 24 July 2024.

40 AECC, *Fuel quality and infrastructure legislation*, 2020, https://www.aecc.eu/legislation/fuel-quality-and-infrastructure-legislation, accessed 1 April 2024.

41 H. Li, Y. Zhang, C. Li, Z. Zhou, X. Nie, Y. Chen, H. Cao, B. Liu, N. Zhang, Z. Said, *et al.*, *Int. J. Adv. Des. Manuf. Technol.*, 2022, **120**, 1–27.

42 P. Tan, Y. Li and H. Shen, *J. Environ. Sci.*, 2017, **55**, 354–362.

43 X. Lyu, X. Liang, Y. Wang, Y. Wang, B. Zhao, G. Shu, H. Tian and K. Wang, *Fuel*, 2024, **366**, 131317.

44 M. J. Plumley, PhD thesis, Massachusetts Institute of Technology, 2005.

45 Driver and Vehicle Licensing Agency, *Get vehicle information from DVLA*, 2024, https://www.gov.uk/get-vehicle-information-from-dvla, accessed 1 April 2024.

46 O. Ghaffarpasand, K. Ropkins, D. C. Beddows and F. D. Pope, *Sci. Total Environ.*, 2023, **858**, 159814.

47 J. Wang, C.-H. Jeong, N. Zimmerman, R. Healy, D. Wang, F. Ke and G. J. Evans, *Atmos. Meas. Tech.*, 2015, **8**, 3263–3275.

48 T. Luan, X. Guo, T. Zhang and L. Guo, *J. Meteorol. Res.*, 2019, **33**, 126–137.

49 F. Amato, M. Schaap, H. A. D. van der Gon, M. Pandolfi, A. Alastuey, M. Keuken and X. Querol, *Atmos. Environ.*, 2012, **62**, 352–358.

This journal is © The Royal Society of Chemistry 2024

Environ. Sci.: Processes Impacts, 2024, **26**, 2145–2157 | **2157**